McGill University

Schulich School of Music

MUMT618

A Matlab Implementation of the Buchla Lopass Gate

Author:
Josh Rohs

Professor:
Dr. Gary Scavone

December 10, 2018

Contents

List of Figures

1 Introduction

The designs of Don Buchla have had a minor resurgence in the past ten years. This can be attributed to a growing interest in analog synthesizers since the late 2000s. Advanced manufacturing technology and user demand drove costs down. Industry heavyweights like Korg (Monotron), DSI (Prophet 08), and Moog (Slim Phatty) released affordable analog synthesisers and birthed the recent boom.

Stemming from this - or at least growing in tandem - has been an explosion in modular synthesizer demand. The popular modular Eurorack format, invented by German company Doepfer in the late 90s, saw more manufacturers enter the fold around this time. Many users preferred the flexibility and heuristic nature of the modular format, forgoing preset sounds for a mutable patch architecture and increased control over sound.

As the collective lens focused on old forms, renewed interest old devices entered the frame. Companies like Verbos and Make Noise took inspiration from the west-coast designs of Buchla and implemented them in the Eurorack standard, providing a new audience for these designs.

Maybe the most influential of the Buchla modules was the 292 Lopass Gate. The gate and its characters tics are defined by its modified Sallen-Key architecture and Vactrol control element - an LED fixed to one or two light dependent resistors in a closed package that provided a rudimentary form of voltage control.

Virtual analog technology has also grown in the last few decades. A lot of research has been done to model the Moog Lowpass filter [4], but considerably less has done to model its west-coast cousin, the Buchla Lopass Gate.

A digital model of the Buchla Lopass gate is explored in a paper of the same name[1], presented by Parker and D'angelo at DAFx 2013 and examined in this report.

2 Audio Circuit

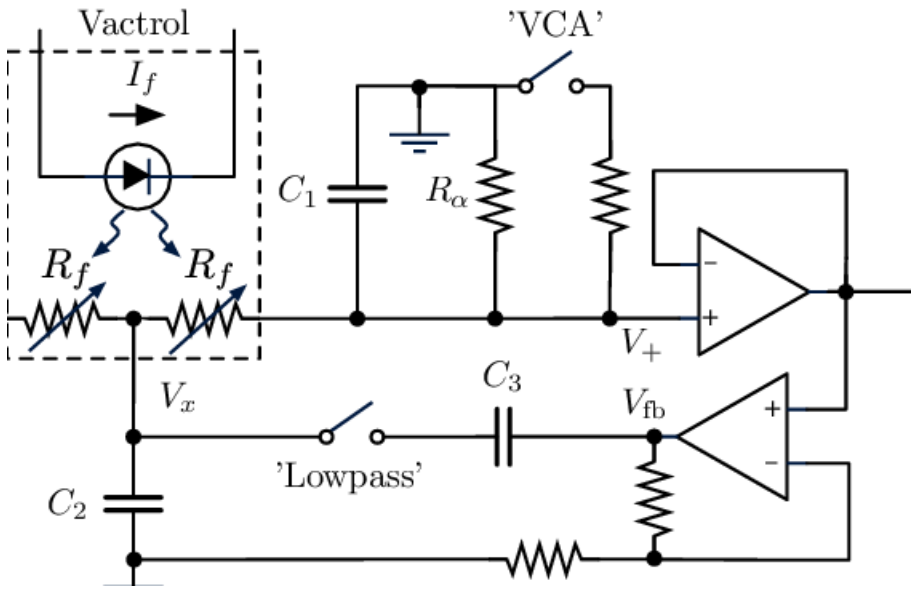

Figure 1: Simplified Buchla Lopass Gate Audio circuit

Parker & D'Angelo present the "canonical" version of the circuit based on recent public domain implementations and original schematics. The audio circuit in the Buchla LPG is responsible for filtering the incoming audio signal. The original circuit(as well as the modified one presented in Figure 1) have 3 operating modes: VCA, Lopass and Both.

VCA, or voltage controlled amplifier mode provides little to no filtering on the input signal. Instead, the volume of the signal is attenuated. The Lopass mode filters the input signal (in the presented model) with adjustable resonance control. The behavior here is complex, since the Q factor is informed by the cutoff control R_f and the resonance, manifesting as a in the transfer function. Also discussed is a nonlinear implementation using diode-clamping feedback, similar to the filter in the Korg MS-20 synthesizer[5].

The Both mode behaves as one would expect and both filters and attenuates the signal. That is, a lower cutoff frequency not only attenuates the high frequencies in the signal, but lowers the overall volume as well. This is a key characters tic in the filters sound, and gives it a percussive nature when modulated with short envelopes or triggers.

The modes are implemented in the original circuit by a multi-pole switch. In the model presented, component values are modified based on the desired mode. This includes changing the value of R_α for VCA and Both mode, and modifying C3 based on whether or not the circuit acts in Lopass mode.

The Buchla LPG audio circuit can be viewed as a modified Sallen-Key topology as seen in figure Figure 2, with the addition of Capacitor C2 and an op-amp buffer in the feedback loop.

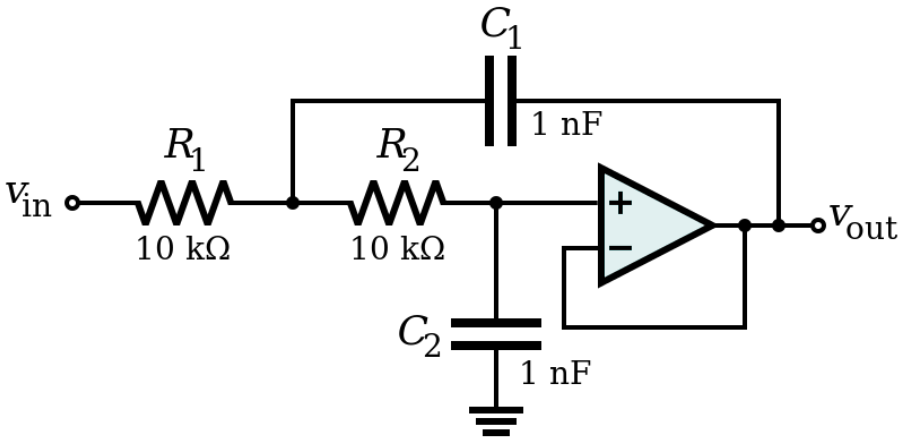

Figure 2: Sallen-Key Filter

2.1 Transfer Function Model

Parker & D'Angelo first model the filter as a second order continuous time transfer function with a variable R_f value. The transfer function is derived by applying nodal analysis to the circuit 1 to derive the following equations:

$$\frac{dV_x}{dt} = b_1 V_{in} + b_2 V_x + b3 V_{out} + b_4 \frac{d}{dt}(d_1 V_{out} + d_2 V_x) \tag{1}$$

$$\frac{dV_{out}}{dt} = a_1 V_x + a_2 V_{out} \tag{2}$$

where

$$a_1 = \frac{1}{C_1 R_f} \qquad b_1 = \frac{1}{C_2 R_f}$$
$$a_2 = -\frac{1}{C_1}(\frac{1}{R_f} + \frac{1}{R_a}) \qquad b_2 = \frac{-2}{C_2 R_f}$$
$$d_1 = \alpha \qquad b_3 = \frac{1}{C_2 R_f}$$
$$d_2 = -1 \qquad b_4 = \frac{C_3}{C_2}$$

Rearranging and taking the Laplace transform, the transfer function is derived as:

$$H_{LPG}(s) = \frac{1}{\alpha_1 + \alpha_2 s + \alpha_3 s^2} \tag{3}$$

where

$$\alpha_1 = 1 + \frac{2R_f}{R_\alpha}$$
$$\alpha_2 = R_f(2C_1 + C_2 - C_3(a-1) + (C_2 + C_3)\frac{R_f}{R_\alpha})$$
$$\alpha_3 = R_f^2 C_1(C_2 + C_3)$$

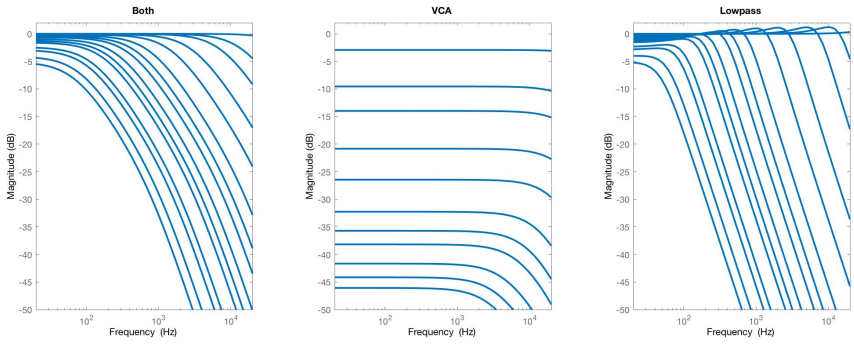

Figure 3: Transfer Function

A plot of the transfer function is shown in figure3 Note that the VCA mode response has a DC gain of -2.92 dB even when fully open. This is due to the loading of the voltage divider between R_f and R_α. It is normally compensated elsewhere in the circuit and thus has not been modeled.

2.2 Discretization

First, a second order Direct form II implementation using the Bilinear transform is proposed. While the behaviour modeled in steady state is accurate, the filter has the potential to be modulated in a way that becomes unstable with the output diverging.

As Parker and D'Angelo note, this is because the transfer function derived from the circuit does not retain system states (in the form of capacitor voltages) one would expect in the form of initial values.

Instead, a version is presented based on the Topology Preserving Transform, or TPT, presented by Zavalishin [2], shown in Figure 4

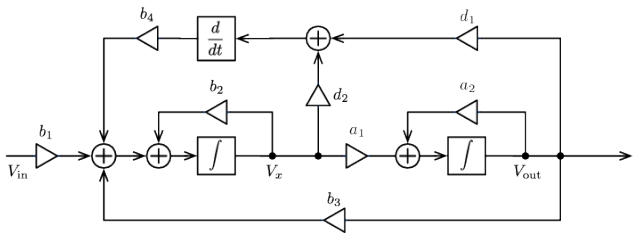

Figure 4: TPT model of the LPG

The block diagrams for each memory element(capacitors) are replaced with their Direct Form II transposed discrete time equivalents as shown in Figure 5. This has the consequence of preserving capacitor states under parameter modulation and maintains stability. An audio example of the filter under heavy modulation is included as "*square2lopasssinenonlinearsmoothedmodel.wav*".

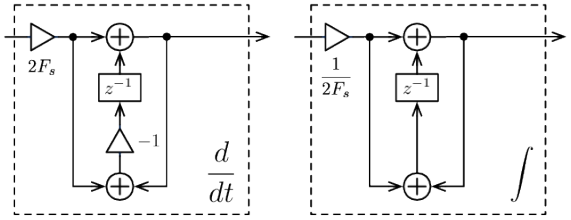

Figure 5: DF II transposed integrator and differentiator

3 Control Circuit

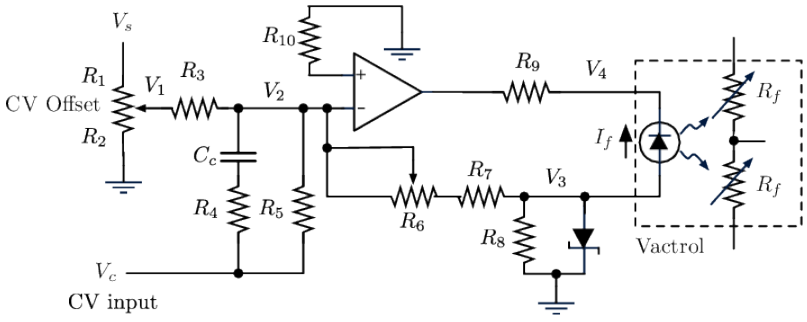

Figure 6: Simplified Buchla LPG Control Circuit

3.1 Transfer function

Applying nodal analysis to the control circuit, Parker & D'Angelo derive the following transfer function piece-wise transfer function for the Vactrol current, I_f

$$\hat{I}_f = \begin{cases} I_{\mathrm{f,min}} & \text{c. 1,} \\ \beta V_3 + \frac{I_\mathrm{a}}{\alpha} & \text{c. 2,} \\ \frac{\gamma G[I_a(R_6+R_7)-V_\mathrm{B}]}{\alpha R_9} - \beta V_\mathrm{B} + \frac{I_\mathrm{a}}{\alpha} & \text{c. 3,} \\ I_{\mathrm{f,max}} & \text{c. 4,} \end{cases} \quad (42)$$

where case 1 corresponds to $I_\mathrm{a} \leq \alpha\left(I_{\mathrm{f,min}} - \beta V_3\right)$,
case 2 to $\alpha\left(I_{\mathrm{f,min}} - \beta V_3\right) < I_\mathrm{a} \leq \frac{V_\mathrm{B}}{R_6+R_7}$,
case 3 to $\frac{V_\mathrm{B}}{R_6+R_7} < I_\mathrm{a} < \frac{\gamma G V_\mathrm{B} + \alpha R_9\left(V_\mathrm{B}\beta + I_{\mathrm{f,max}}\right)}{\gamma G(R_6+R_7)+R_9}$,
and case 4 to $I_\mathrm{a} \geq \frac{\gamma G V_\mathrm{B} + \alpha R_9\left(V_\mathrm{B}\beta + I_{\mathrm{f,max}}\right)}{\gamma G(R_6+R_7)+R_9}$.

Figure 7: Piecewise I_f transfer function[1]

The approximation is plotted along with results of a SPICE simulation of the circuit. It should be noted that the function contains a correction factor, γ of 0.001. It should also be noted that there is a hard knee in the IV curve based on the piecewise nature of the function as seen in Figure 8.

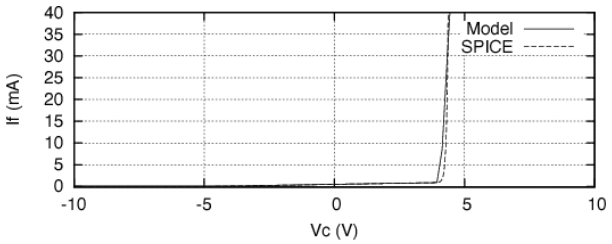

Figure 8: Control Circuit IV-Curve [1]

Figure 9 depicts the spectrum of a Square wave filtered by the Parker-D'angelo model when the control voltage is linear swept from 0V until the op-amp saturates (40mA of output current) in 2 seconds before immediately dropping to 0V. From the graph and the audio file "square2 both sweep nonlinear pd model.wav" attached to this report, one can determine that this is not ideal. The steep slope creates a less useful range of control voltage and the hard knee creates a range in the response that doesn't really sound like the Lopass gate frequency response.

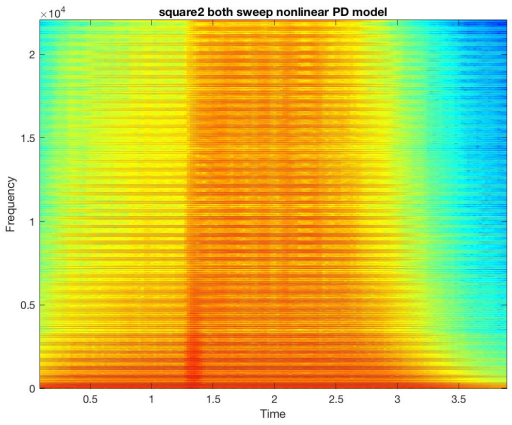

Figure 9: Spectrum of a linear Sweep with PD I-V function

To verify this, a quick test was performed. The results are exhibited in a spectrogram of a sweep of a real Lopass gate (Make Noise QMMG). It's clear that the knee region is smoother and allows for a less discontinuous jump when control voltages are swept.

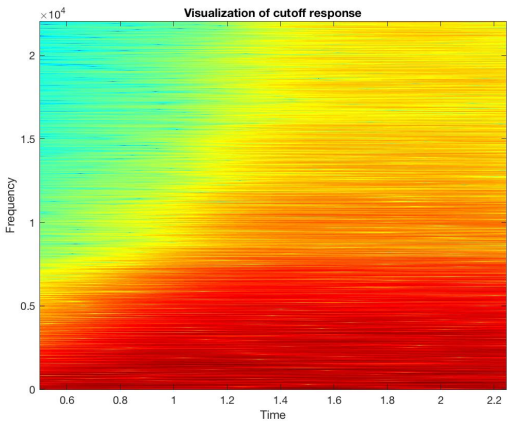

Figure 10: Spectrum of an analog LPG to linear CV sweep

To rectify any artifacts presented in the smoothing of the IV curve, one could substitute the Parker-D'angelo Model for a smoother Curve. A tuned I-V curve is presented in Figure 11.

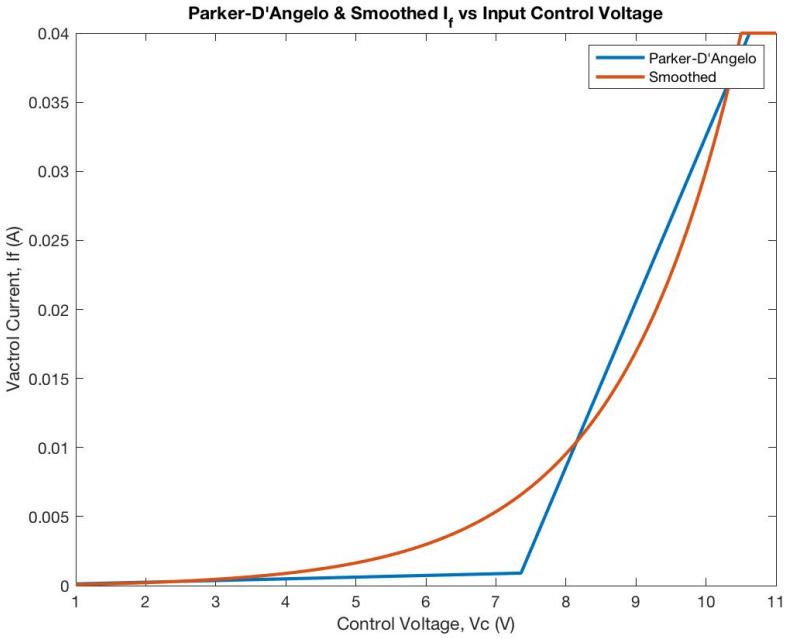

Figure 11: Parker D'Angelo and Smoothed I-V curve

The smoothed curve is based on a modified Shockley-Diode equation

$$I_f = Is(e^{\frac{Vc\beta}{nv_t}} - 1) \tag{4}$$

Where I_s is the minimum forward current and β is a parameter chosen to approximate the response range giving 40mA for around 10V input. V_c is the control voltage input, n is a

diode constant taken from the Parker-D'Angelo paper and V_T is the thermal voltage at room temperature(26mV).

A spectrogram of the result(using the same parameters as Figure 9) is shown in Figure 12. Two audio examples - one in each mode - are attached as "*square_both_sweep_nonlinear_PD_model.wav*". "*square_both_sweep_nonlinear_smoothed_model.wav*".

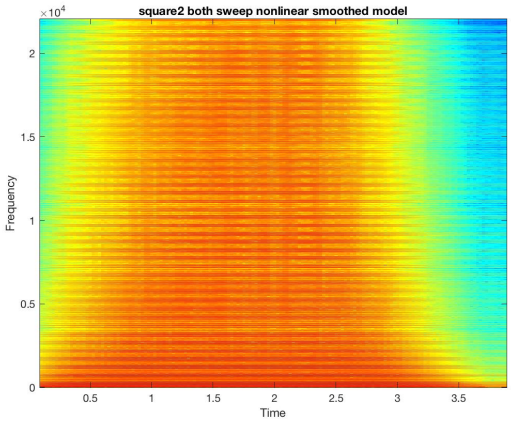

Figure 12: Spectrum of Linear sweep with smoothed IV-curve

3.2 Vactrol Model

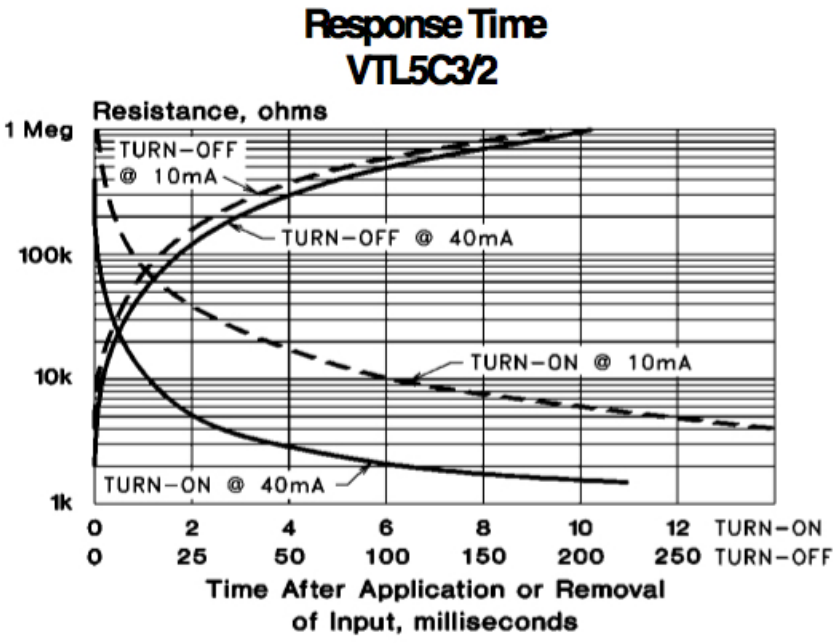

Figure 13: Vactrol Turn-Off/Turn-On Time[3]

The Vactrol control of the audio circuit cutoff is another key component to the Low Pass Gate sound. An important characteristic that distinguishes it from other methods of voltage control

is the variable response time of the Vactrol. As seen in Figure 13, the "turn-on" time is relatively short while the "turn-off" time usually an order of magnitude longer.

We can model the vactrol response using a time-variant implementation based on a one pole filter. To get the response time, we must calculate the desired filter cutoff frequency. We can use the analog cutoff value, ω_c, to determine the time constant of the filter.

The approximation

$$t_{decay} \approx 5\tau = \frac{5}{w_c} \tag{5}$$

In other words,

$$w_c \approx \frac{5}{t_{decay}} \tag{6}$$

Using the Perkin Elmer VTL5C3/2 Datasheet [3], we can determine nominal cutoff values of 20 Hz and 400 HZ for 250 ms and 12.5 ms, respectively.

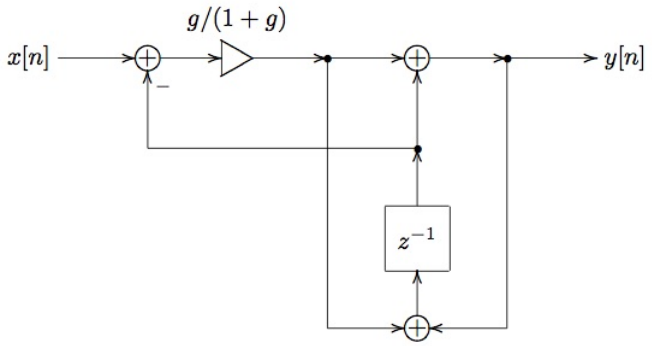

Figure 14: Zero-feedback One Pole Filter [2]

In order to get the appropriate "slurring" (in this case, filtering) of control voltages, we implement a one pole filter using the topology discussed by Zavalishin [2] in figure 14

The gain g in Figure 1 is the continuous time cutoff frequency obtained above scaled by twice the sampling rate ($\frac{\omega_c}{2Fs}$).

CV effect on Attack/Decay

One other characteristic of the Vactrol response is the fact that the "attack" and "decay" times of the Vactrols "envelope" are determined by the level of the vactrol current, I_f. For example, A higher control voltage(and therefore, current) will result in a quicker rise time and a slower decay time. The Parker-D'angelo model includes feedback from the output to scale the filter cutoff but the implementation's effects are fairly minimal.

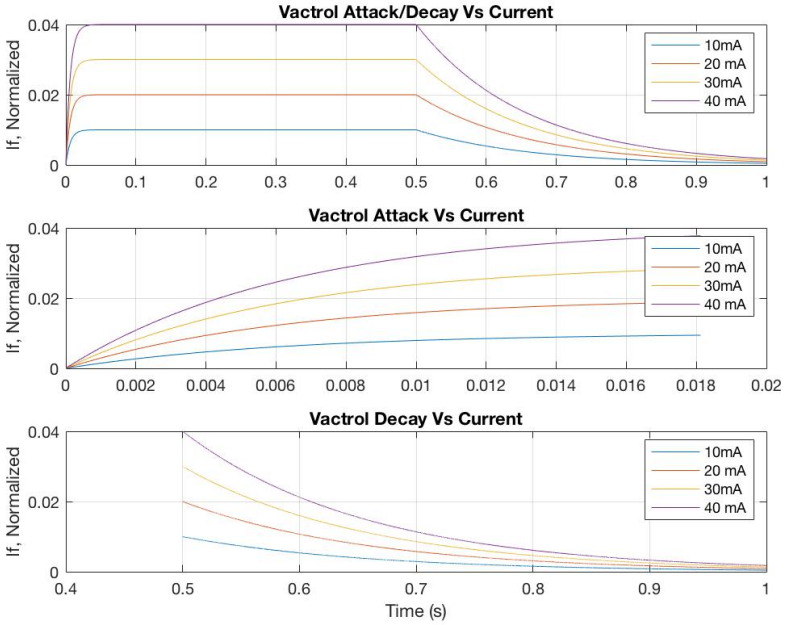

Figure 15: P-D Vactrol A/D Curve

Figure 15 shows the response for a short current pulse of varying levels. Figure 16 shows the normalized version of these curves (dividing the output by the input amplitude). The actual time constant of the exponential response does not change noticeably between different levels. To exaggerate the effect, new user parameters, ρ_{on} and ρ_{off} are presented in the Matlab code below.

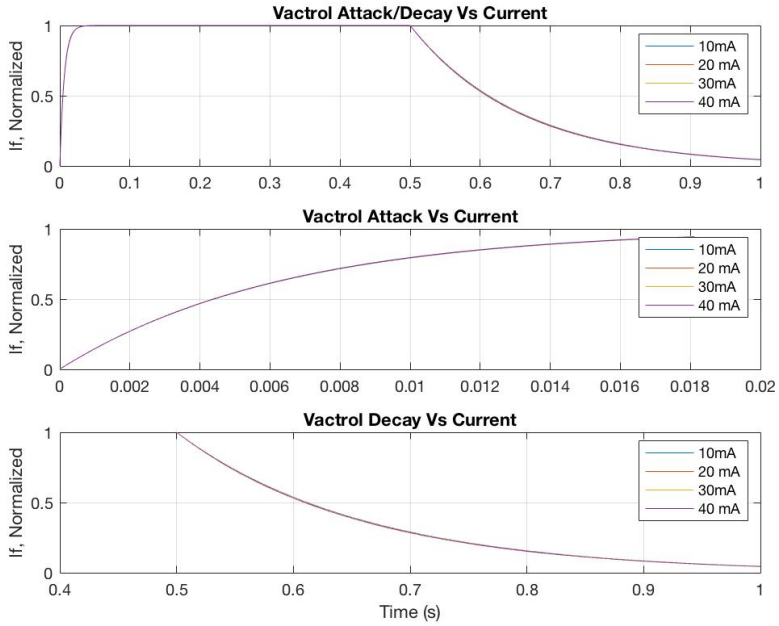

Figure 16: Normalized P-D Vactrol A/D Curve

By parameterizing the level of attack/decay variation with ρ_{on} and ρ_{off}, the user can decide the difference in slewing between a high control current and a low one. This is useful when an accent is used to emphasize certain notes. The formula is normalized to provide the decay/attack time set by the user when a maximum 40mA current pulse is sent to the control circuit and the user parameter ρ is set to 0. By allowing rho values to be negative, the natural behavior of the control element can be reversed so that a higher pulse decays quicker than a lower one.

```
dir = sign(If(i)-x_m1);
if dir ~= dir_n1
%Only update when input direction is changed
    switch(dir)
        case 1
            wc = wc_on*(1-rho_on+rho_on*If(i)/.040);
            % Use incoming cv_in value to scale cutoff based on max
        case 0
            %wc = wc;
        case -1
            wc = wc_off*(1+rho_off-(rho_off)*(yc)/0.040)
            % use outgoing yo value to scale cutoff based on max cu
        otherwise
            display("This shouldn't print");
    end
end
```

In Figure 17 and Figure 18, two plots showing response times for different ρ_{on} and ρ_{off} values are shown. It is clearly a more drastic effect than the original model. An audio example demonstrating this is attached as "$rho_90_trigger.wav$".

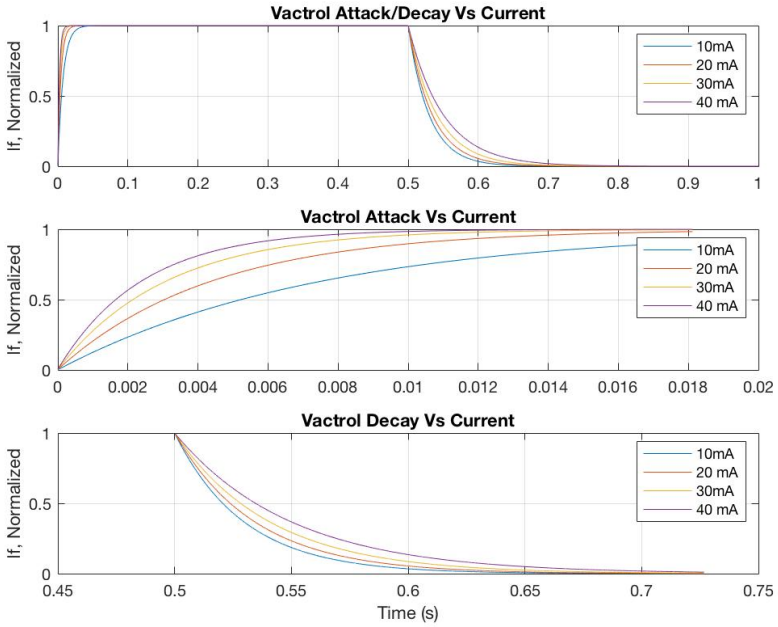

Figure 17: Vactrol curve for ρ_{on} and ρ_{off} both set to 0.9

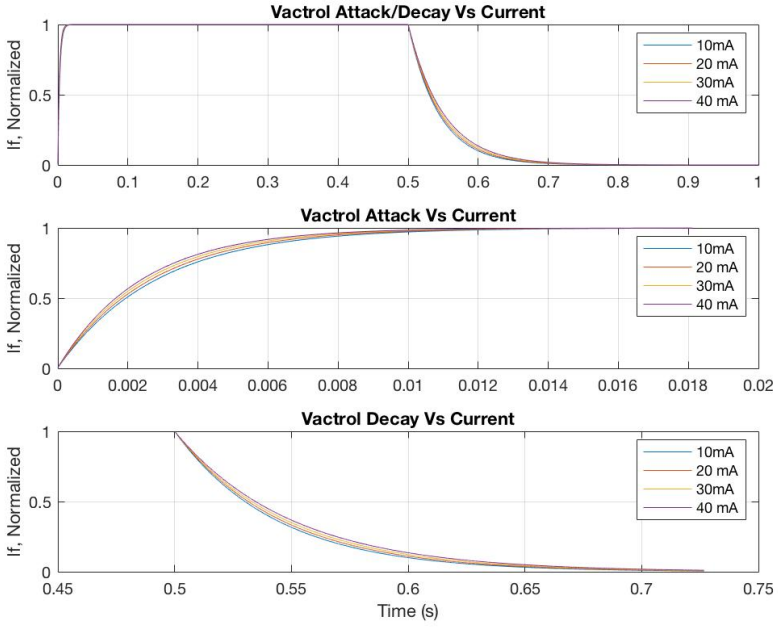

Figure 18: Vactrol curve for ρ_{on} and ρ_{off} both set to 0.2

In the "wild", each manufactured Vactrol has a differing nonlinear response. Between in-

cluding controls for global on/off response time and level-depended variation, this model allows the user to mimic the behavior of any Vactrol they want. This is different than the MAX/MSP patch accompanying Parker & D'Angelo's paper.

Conclusions

The attached Matlab scripts comprise a digital implementation of the Buchla Low Pass Gate based on the one presented by Parker & D'Angelo. The model is stable under modulation and allows the user to tweak parameters related to the Vactrol response, which is not present in the original. Firstly, the nominal Vactrol attack/decay times can be set by the user. This is preferable to using fixed times as it allows the user more flexibility over the LPG's sound while still retaining the characteristic behavior. One could also, for example, automate attack/decay time to create sonic movement or even extend the vactrol "ring" time beyond those found naturally to expand the timbral palette.

Also added to the Matlab model are the ρ parameters which allow for control over how the level affects the decay time.

With a minimal amount of optimization, the model presented could be implemented in realtime using STK and/or JUCE or,ideally, ported to an embedded environment with eurorack specifications to take advantage of the additional modulatable parameters introduced here. Because vactrol elements are increasingly scarce, this allows for an implementation that is independent of increasingly long procurement times and inflated prices associated with the endangered component.

Attachments

$MUMT618_buchla\_lpg.m$,
$getCv.m$,
$getCurrent.m$
"$rho\_trigger\_90.wav$" $square2\_both\_sweep\_nonlinear\_pd.wav$
$square2\_both\_sweep\_nonlinear\_smooth.wav$
"$myspecgram.m$"

References

[1] Julian Parker & Stefano D'Angelo, *A Digital Model of the Buchla Lowpass-Gate,* in *Proc. of the 16th Int. Conference on Digital Audio Effects (DAFx-13), Maynooth, Ireland, September 2-6, 2013*

[2] V. Zavalishin, *The Art of VA Filter Design, Native Instruments, Berlin, Germany, 2012.*

[3] Perkin Elmer Optoelectronics, Photoconductive Cells and Analog Optoisolators (Vactrols), 2001.

[4] T. Stilson and J. O. Smith, *Analyzing the Moog VCF with considerations for digital implementation, in Proc. Int. Computer Music Conf., Hong Kong, Aug. 1996, pp. 398 401.*

[5] T. E. Stinchcombe, *A Study of the Korg MS10 & MS20 Filters,* 2006.